ARTICLE
Journal of Cellular Biochemistry 116:598–608 (2015)

Journal of Cellular Biochemistry

MicroRNA-29b Inhibits Migration and Proliferation of Vascular Smooth Muscle Cells in Neointimal Formation

Jiyun Lee,[1,2] Soyeon Lim,[3] Byeong-Wook Song,[4] Min-Ji Cha,[5] Onju Ham,[1,2] Se-Yeon Lee,[1,2] Changyoun Lee,[1,6] Jun-Hee Park,[5] Yoonjin Bae,[1] Hyang-Hee Seo,[1,2] Minji Seung,[1,2] Eunhyun Choi,[5,7] and Ki-Chul Hwang[5,7]*

[1]*Cardiovascular Research Institute, Yonsei University College of Medicine, Seoul 120-752, Republic of Korea*

[2]*Brain Korea 21 PLUS Project for Medical Science, Yonsei University College of Medicine, Seoul 120-752, Republic of Korea*

[3]*Severance Integrative Research Institute for Cerebral & Cardiovascular Disease, Yonsei University Health System, Seoul 120-752, Republic of Korea*

[4]*EIT/LOFUS R&D Center, Institute of Medical Industrialization, International St. Mary's Hospital, Incheon 404-834, Republic of Korea*

[5]*Institute for Bio-Medical Convergence, College of Medicine, Catholic Kwandong University, Gangneung-si, Gangwon-do 210-701, Republic of Korea*

[6]*Department of Integrated Omics for Biomedical Sciences, Graduate School, Yonsei University, Seoul 120-749, Republic of Korea*

[7]*Catholic Kwandong University International St. Mary's Hospital, Incheon, 404-834, Republic of Korea*

ABSTRACT

The proliferation and migration of smooth muscle cells (SMCs) are considered to be key steps in the progression of atherosclerosis and restenosis. Certain stimuli, such as, interleukin-3 (IL-3) are known to stimulate proliferation and migration in vascular diseases. Meanwhile, microRNAs (miRs) have been revealed as critical modulators of various diseases in which miR-29b is known to regulate cell growth by targeting Mcl-1 and MMP2. However, roles of miR-29b in vascular smooth muscle cells remain almost unknown. We hypothesized that miR-29b may control the proliferation and migration processes induced by IL-3 stimulation by inhibiting its own specific targets in SMCs. MiR-29b significantly suppressed the proliferation and migration of SMCs through the inhibition of the signaling pathway related to Mcl-1 and MMP2. We also found that miR-29b expression levels significantly declined in balloon-injured rat carotid arteries and that the overexpression of miR-29b by local oligonucleotide delivery can inhibit neointimal formation. Consistent with the critical role of miR-29b in vitro, we observed down-regulated expression levels of Mcl-1 and MMP2 from the neointimal region. These results indicate that miR-29b suppressed the proliferation and migration of SMCs, possibly through the inhibition of Mcl-1 and MMP2, and suggest that miR-29b may serve as a useful therapeutic tool to treat cardiovascular diseases such as, atherosclerosis and restenosis. J. Cell. Biochem. 116: 598–608, 2015.

KEY WORDS: SMOOTH MUSCLE CELL; PROLIFERATION; MIGRATION; MicroRNA-29b

Jiyun Lee and Soyeon Lim contributed equally to this work.
Conflicts of interest: None.

Grant sponsor: Korean Government (MEST); Grant number: 2014030459; Grant sponsor: Ministry of Health & Welfare, Republic of Korea; Grant number: A120478; Grant sponsor: Yonsei University College of Medicine; Grant number: 8-2012-0015.

*Correspondence to: Prof. Ki-Chul Hwang, PhD, Institute for Bio-Medical Convergence, College of Medicine, Catholic Kwandong University, Gangneung-si, Gangwon-do, 210-701, Korea. E-mail: kchwang@ish.or.kr/kchwang@cku.ac.kr

Manuscript Received: 11 April 2014; Manuscript Accepted: 28 October 2014
Accepted manuscript online in Wiley Online Library (wileyonlinelibrary.com): 11 November 2014
DOI 10.1002/jcb.25011 • © 2014 Wiley Periodicals, Inc.

Restenosis is the recurrence of stenosis and involves a re-blockage of a reperfused vessel that was initially inflamed due to endothelial cell damage [Smith, 2002] followed by proliferation and migration of smooth muscle cells (SMCs) [Costa and Simon, 2005], this process is overlooked by numerous proinflammatory cytokines and growth factors. One type of cytokine, interleukin-3 (IL-3), is an important signal produced by activated T-cells and plays critical roles in inflammation and the immune response [Voehringer, 2012]. IL-3 levels have been shown to be significantly higher in patients with coronary artery disease or in patients with restenosis versus patients without restenosis [Rudolph et al., 2009]. IL-3 was also observed to increase the migration and proliferation rates of SMCs in human atheroma [Brizzi et al., 2001]. There are many other important factors that stimulate proliferation and migration, butIL-3 induced phenomenon has not been well investigated in the pathophysiology of SMCs.

Once SMCs recognize an IL-3 cytokine through the IL-3 receptor, several signaling pathways related to proliferation and migration are activated. The activation of ERK1/2 mitogen-activated protein kinase (MAPK) and phosphatidylinositol-3 kinase (PI3K)-Akt pathways are the most well-known among these. The activation of these pathways can cause an increase in myeloid cell leukemia sequence 1 (Mcl-1) expression and activate matrix metalloproteinases (MMPs) [Brizzi et al., 2001; Steele et al., 2010].

Up to date, microRNAs (miRs) have been extensively studied as a powerful therapeutic tool for the treatment of many diseases such as, cancers [Kasinski and Slack, 2012], neurodegenerative diseases [Lee et al., 2012], and autoimmune diseases [Bernecker et al., 2012], and even as a regulator for differentiation and regeneration [Kwon et al., 2005; Ounzain et al., 2012]. With respect to cardiovascular diseases, several microRNAs have also been revealed to be highly involved in arterial remodeling [Kairouz et al., 2012; Wang et al., 2012b]. MiR-21, miR-1, miR-145, and miR-221/222 are especially well-known for their roles related to cytokines and growth factors in the proliferation and migration of SMCs [Fichtlscherer et al., 2010; McDonald et al., 2012; Nazari-Jahantigh et al., 2012].

Studies related to the miR-29 family have demonstrated that miR-29, especially miR-29b, is important for tumor suppression by regulating proliferation and migration through the suppression of SPARC and COL4A2 [Schmitt et al., 2012; Wang et al., 2012a]. Several reports have demonstrated miR-29b regulation of abdominal aortic aneurysm, vascular calcification, and migration/proliferation through the targeting of different targets such as, collagens, ADAMTS-7, and PDGFR [Du et al., 2012; Maegdefessel et al., 2012; Talasila et al., 2013]. Various targets of miR-29b are known in vascular diseases, but little is known about the mechanisms of miR-29b related to Mcl-1 and MMPs in SMC proliferation and migration, especially restenosis.

Therefore, we hypothesized that miR-29b regulates the IL-3-induced proliferation and migration of SMCs through its putative gene targets, which can affect vascular smooth muscle remodeling and may be useful as a tool for novel molecular therapy.

MATERIALS AND METHODS

MATERIALS

Dulbecco's modified eagle's medium (DMEM), fetal bovine serum (FBS), and penicillin-streptomycin were obtained from Gibco BRL (Grand island, NY). Recombinant rat interleukin-3 was obtained from R&D Systems (R&D Systems Inc., MN). Rno-miR-29b and Cyanine Dye3 (Cy3)-labeled miR-29b were purchased from Genolution Pharmaceuticals and Bioneer (Daejeon, Korea), respectively. The antibodies of Mcl-1and MMP9 were purchased from Abcam. Antibodies of MMP2, ERK, phospho-ERK, PCNA (PC10), and Cy3 (A-6) were purchased from Santa Cruz Biotechnology (Santa Cruz, CA). Antibodies of Akt and phospho-Akt were purchased from Cell Signaling (Danvers, MA).

ANIMAL

All experimental procedures for animal studies were approved by the Committee for the Care and Use of Laboratory Animals, Yonsei University College of Medicine, and performed in accordance with the Committee's Guidelines and Regulations for Animal Care. Sprague-Dawley rats were anesthetized by intramuscular administration of 20 mg/kg Tiletamine-Zolazepam and 5 mg/kg Xylazine hydrochloride. The depth of anesthesia was confirmed by the toe-pinch reflex procedure and absence of muscular tone, a commonly used method in monitoring the depth of anesthesia.

ISOLATION AND CULTURE OF RAT AORTIC SMOOTH MUSCLE CELLS

Rat aortic smooth muscle cells (RAoSMCs) were isolated from the thoracic aortas of 6–8-week-old Sprague–Dawley rats as previously described [Hwang et al., 2002]. Briefly, after administering anesthesia, the thoracic aortas of SD rats were removed and transferred on ice in serum-free DMEM. The aorta was freed from connective tissue, transferred into a Petri dish containing 5 ml of an enzyme dissociation mixture containing DMEM with 1 mg/ml of collagenase type I (Sigma-Aldrich Inc., St. Louis, MO) and 0.5 mg/ml elastase (USB Bioscience, Cleveland, OH), and incubated for 30 min at 37 °C. The aorta was then transferred into DMEM, and the adventitia was stripped off with forceps under a binocular microscope. The aorta was transferred into a plastic tube containing 5 ml of the enzyme dissociation mixture and incubated for 2 h at 37 °C. The suspension was centrifuged at 1,500 rpm for 10 min and the pellet was resuspended in 10% FBS DMEM. RAoSMCs were cultured in 10% FBS DMEM at 37 °C and 5% CO_2. Experiments were performed using RAoSMCs between passages four and nine.

CELL PROLIFERATION ASSAY

SMCs were plated in triplicate wells of 96-well plates at 2×10^3 cells/well. The cells were pretreated with 0.1% FBS DMEM for 48 h and then treated with IL-3 (80 ng/ml) for 48 h. After treatment, MTT [3-(4,5-dimethylthiazol-2-yl)-2,5-diphenyl-2H-tetrazoliumbromide] solution (Dojindo, Osaka, Japan) at a final concentration of 0.5 mg/ml was added to each well and incubated at 37 °C for 2 h to allow MTT reduction. The absorbance of the samples was measured at 450 nm using a microplate reader.

CELL MIGRATION ASSAY

The effect of IL-3 on the migration of SMCs was examined by performing a modified Boyden chamber assay in Transwell cell culture chambers (Nunc, Rochester, NY). SMCs were transfected with miR-29b, put under starvation with 0.1% FBS DMEM for 24 h and then treated with IL-3 for 12 h. SMCs were suspended in 0.1% FBS DMEM. Then, 10% FBS DMEM was added to the lower chamber and the cells were incubated for 9 h at 37 °C. Cells that migrated beneath the filter were fixed in methanol and stained with hematoxylin. Five randomly chosen fields were counted at 200x magnification with an inverted microscope.

WOUND-HEALING ASSAY

For the wound-healing assay, a rectangular lesion was created using a cell scraper. The cells were then rinsed with serum-free DMEM and incubated with IL-3 for 48 h. After the designated times, three randomly selected fields at the lesion border were acquired using a CCD camera (Olympus, Japan). In each field, the distances from the margin of the lesion to the most migrated cells were measured, and the mean value of the distances was taken as the mobility value of the cells in each culture dish.

AORTIC RING ASSAY

Ex vivo migrations of SMCs were measured by an aortic ring assay using Matrigel with some modifications. This method was described by Baker et al. [2012]. After administering anesthesia, the adventitia of the aortas of six-week-old Sprague–Dawley rats was removed enzymatically using collagenase (Sigma-Aldrich Inc., St. Louis, MO), and endothelia were removed by scraping the interior surfaces with forceps. The vessels were then cut into 1 mm rings. The rings were placed and embedded in 48-well plates coated with 120 μl Matrigel (BD Biosciences, San Jose, CA), which were then overlaid with an additional 50 μl Matrigel. The aortas were pretreated with serum-free DMEM for 24 h and then transfected with 100 nM miR-29b under transfection conditions. After 12 h, IL-3 (80 ng/ml) in 10% FBS DMEM was added. Culture media were changed every two days, and aortic rings were examined every two days. Using the NIH Image J version 1.34e software, digital images were taken at 14 days for quantitative analysis of vascular SMC outgrowth.

IMMUNOBLOT ANALYSIS

The cells were washed in PBS and lysed in a lysis buffer (Cell Signaling, Danvers, MA). Protein concentrations were determined using the BCA Protein Assay Kit (Thermo Fisher Scientific Inc., Waltham, MA). Proteins were separated in a sodium dodecyl sulfate-polyacrylamide gel and transferred to a polyvinylidenedifluoride membrane (Millipore, Billerica, MA). After blocking the membrane, the membranes were incubated with primary antibodies overnight at 4 °C. The membrane was washed three times with TBS-T for 10 min and then incubated with horseradish peroxidase-conjugated secondary antibodies at room temperature for 1 h. After extensive washing, the bands were detected by an enhanced chemiluminescence reagent (Santa Cruz Biotechnology, Santa Cruz, CA). The band intensities were quantified using NIH Image J version 1.34e software.

RT-PCR ANALYSIS

The expression levels of various genes were analyzed by reverse transcription polymerase chain reaction (RT-PCR). Total RNA was extracted from 60 mm plates using 500 μl TRIzol® reagents (Sigma-Aldrich Inc., St. Louis, MO). 100 μl chloroform was added to each sample and vortexed for approximately 10 s. The samples were then centrifuged at 12,000 rpm at 4 °C for 15 min. Of the three resulting layers, the upper transparent layer was collected in a new tube. Thereafter, 300 μl 2-propanol was added to the sample, and the mixture was inverted for approximately 10 s before centrifugation at 12,000 rpm at 4 °C for 10 min. Next, the pellet was washed with 75% ethanol mixed with diethylpyrocarbonate (DEPC; Sigma-Aldrich Inc., St. Louis, MO) in water. The pellet was centrifuged again at 12,000 rpm at 4 °C for 5 min and then dried at room temperature. Finally, 30 μl of nuclease-free water was added. The RNA quality and quantity were determined based on the OD_{260}/OD_{280} using a DU 640 spectrophotometer (Eppendorf AG, Hamburg, Germany).

Complementary DNA (cDNA) was generated with the Promega (Fitchburg, WI) Reverse Transcription System according to the manufacturer's instructions. One microgram of total RNA was reverse-transcribed in a 20 μl reaction volume containing 5 mM $MgCl_2$, 10 mM Tris-HCl (pH 9.0 at 25 °C), 50 mM KCl, 0.1% Triton X-100, 1 mM dNTP mix, 20 U RNase inhibitor, 0.5 μg oligo-(dT) 15 primer, and 10 U reverse transcriptase for 15 min at 42 °C. The reaction was terminated by heating at 99 °C for 5 min. The PCR mix contained 10 mM of each primer, together with 200 mM Tri-HCl (pH 8.8), 100 mM KCl, 1.5 mM $MgSO_4$, 1% Triton X-100, 0.1 mM dNTP mix, and 1.25 U Taqpolymerase in a total volume of 25 μl. PCR conditions consisted of denaturing at 94 °C for 3 min, followed by 35 cycles of denaturation at 94 °C for 30 s, annealing at 94 °C for 30 s, and extension at 72 °C for 30 s before a final extension at 72 °C for 10 min. RT-PCR products were separated by electrophoresis on a 1.2% agarose gel (Bio-Rad, Hercules, CA). A Gel-Doc (Bio-Rad, Hercules, CA) was used to visualize the bands after staining with ethidium bromide.

microRNA TRANSFECTION

Transfections of microRNA were performed using a siLentFact reagent. Briefly, cells were seeded at a density of 2×10^5 cells per 35 mm culture plate. The siLentFact reagent was diluted with Opti-MEM and combined with its indicated microRNA mimic per plate. The microRNA and siLentFact reagent were added to each plate containing fresh medium and cells. After 4 h incubation in a CO_2 incubator at 37 °C, the medium was changed to 10% FBS DMEM.

REAL-TIME POLYMERASE CHAIN REACTION (PCR)

Total RNA was isolated with TRIzol® reagent (Sigma-Aldrich Inc., St. Louis, MO). Briefly, 100 ng purified total RNA was used for reverse transcription (TaqMan® MicroRNA Reverse Transcriptase Kit, [Applied Biosystems, Foster City, CA]) in combination with the TaqMan® MicroRNA Assays for the quantification of specific microRNAs and U6 control transcripts, according to the manufacturer's conditions. The amplification and detection of specific

products were performed in a Light Cycler 480 II (Roche, Upper Bavaria, Germany) at 95 °C for 10 min, followed by 40 cycles at 95 °C for 15 s, and 60 °C for 60 s. The threshold cycle (Ct) of each target gene was automatically defined and was located in the linear amplification phase of the PCR and normalized to the U6 (ΔCt value) of each group. The relative difference in expression levels of microRNAs in the cells (ΔΔCt) was calculated and presented as fold induction ($2^{-\Delta\Delta Ct}$).

LUCIFERASE ASSAY

A public database (TargetScan. www.targetscan.org) was searched for the predicted target gene of miR-29b. We synthesized the 3′-UTRs of *Mcl-1* and *MMP2* that contained the binding site of miR-29b. The corresponding gene was then cloned into the pmirGLO vector. HeLa cells were used for transfection. After 48 h, the pmirGLO vector containing the *Mcl-1* and *MMP2* binding sites for miR-29b was co-transfected with miR-29b or the negative control using Lipofectamine 2000 (Thermo Fisher Scientific Inc., Waltham, MA). Renilla luciferase was used for normalization. Luciferase activity was measured with the Dual Luciferase assay (Promega, Fitchburg, WI) according to the manufacturer's instructions after 48 h on a luminometer (Promega, Fitchburg, WI).

CAROTID ARTERY BALLOON INJURY MODEL

After administering anesthesia, the left common carotid artery of eight-week-old SD rats was exposed by cervical midline excisions. The proximal portion of the left common carotid artery and the origin of the left internal carotid artery were temporarily ligated with surgical threads to prevent excessive bleeding during the balloon catheter insertion. Part of the external carotid artery wall was excised for a 2-Fr Fogarty balloon catheter (Baxter Healthcare Corp., Irvine, CA) insertion. After the insertion of the balloon catheter, the temporarily ligated proximal left common carotid artery was untied and the catheter was advanced in the direction of the ascending aorta. The balloon was inflated just enough to develop a mild resistance against the arterial wall (0.2 ml). The expanded balloon catheter was then pulled back to inflict uniform injury along the entire common carotid artery wall. This procedure was repeated three times for the complete denudation of the intima, after which the catheter was removed and the proximal external carotid artery was ligated. Sham operations were performed on the right common carotid arteries.To analyze neointimal proliferation, neointimal (I) and medial (M) area, NIH Image J version 1.34e software was used. From the enclosed area by external elastic lamina (EEL), internal elastic lamina (IEL), and vessel lumen (VL), the neointimal (I) and medial (M) area were calculated from the (IEL-VL) and (EEL-IEL), respectively [Kumar et al., 1997].

LOCAL OLIGONUCLEOTIDE DELIVERY INTO VASCULAR WALLS

To deliver the control microRNA, miR-29b, or Cyanine Dye3 (Cy3)-labeled miR-29b to the vascular tissue, we applied an established local oligonucleotide delivery model via F-127 pluronic gel (Sigma-Aldrich Inc., St. Louis, MO) as described by Xiaojun Liu et al [Liu et al., 2011]. Immediately after balloon injury of the right common carotid artery, transfection solution (50 μl 0.2% transfection reagent in Opti-MEM) was mixed with control microRNA, miR-29b, or Cy3-miR-29b (10 μg) and infused into the ligated segment of the common carotid artery for 30 min. Then, 90 μg of these microRNAs, preloaded into 200 μl 30% F-127 pluronic gel and 1% transfection reagent at 4 °C, was applied locally to the adventitia around the injured artery segments.

FLUORESCENCE INTENSITY

Cy3-labeled miR-29b was transfected into the vascular walls using the local oligonucleotide delivery system. The vessels were perfusion-fixed overnight with 10% (v/v) neutral-buffered formaldehyde, transversely sectioned into serial thick sections, and embedded in paraffin using routine methods. Sections 2 μm thick were mounted on gelatin coated glass slides to ensure that different stains could be used on successive sections of the tissue. After deparaffinization, the sections were analyzed with DAPI and Cy3-miR-29b by an optical in vivo imaging system spectrum (IVIS; Caliper Life Science, Hopkinton, MA) and confocal laser scanning microscope LSM700 (Carl Zeiss, Thornwood, NY). Cy3-miR-29b from isolated carotid arteries was detected by the optical in vivo imaging system spectrum.

IMMUNOFLUORESCENCE

Perfused vessels were fixed overnight with 10% (v/v) neutral-buffered formaldehyde, transversely sectioned into serial thick sections, and embedded in paraffin using routine methods. Sections 2 μm thick were mounted on gelatin coated glass slides to ensure that different stains could be used on successive sections of tissue cut through the areas of balloon injury. After deparaffinization, rehydration, and rinsing with PBS, sodium citrate antigen retrieval was performed using 10 mM sodium citrate (pH 6.0) in a microwave for 10 min. Sections were incubated in 1% H_2O_2 for 10 min to quench endogenous peroxidase. To remove flavin coenzyme auto fluorescence, tissue sections were treated with 0.1% sodium borohydride for 30 min. Samples were blocked in 2.5% normal horse serum and incubated in primary antibody overnight. The sections were analyzed with DAPI, Mcl-1, MMP2, PCNA, and Cy3 by confocal laser scanning microscope LSM700 (Carl Zeiss, Thornwood, NY).

HISTOLOGY

To measure the neointimal areas, aortas were excised from sacrificed rats and perfused with phosphate buffered saline (PBS) to remove blood and then fixed in 10% formalin solution for 24 h at 4 °C. Sequentially, tissue sections were mounted onto gelatin-coated glass slides to guarantee that different stains could be used on successive tissue sections cut through the injury area. After the sections were deparaffinized and rehydrated, they were stained with hematoxylin and eosin (H&E) to estimate neointimal areas and quantified using NIH Image J software version 1.34e. Collagen was also analyzed using Masson's Trichrome staining.

ZYMOGRAPHY

The enzyme activities of MMPs were assessed by gelatin zymographic analysis. The conditioned medium was collected and protein concentration was measured with a BCA protein assay. Approximately 25 μg proteins was loaded onto 10% SDS-PAGE gels containing 0.1% gelatin and electrophoretically separated in a 4 °C

cold room. Subsequently, gels were washed using renaturing buffer and were incubated with enzyme activation buffer for 20 h at 37 °C, stained with 0.25% Coomassie brilliant blue, destained with 50% methanol in 40% acetic acid. The zymograms were photographed on a light box, and proteolysis was detected as a white zone against a blue background.

STATISTICAL ANALYSIS

All experiments were performed in triplicate. Data are expressed as means ± SE. The statistical analysis of two groups was estimated by Student's *t*-test. Comparisons of more than two groups were completed by one-way ANOVA using the Bonferroni test. $P < 0.05$ was considered significant.

RESULTS

IL-3 INDUCED SMC PROLIFERATION AND MIGRATION

To confirm the effect of IL-3 on the proliferation and migration of SMCs, an MTT assay and modified Boyden chamber assay were performed under IL-3 stimulation. Concentrations of 20–100 ng/ml of IL-3 were applied for 48 h to determine an optimal IL-3 concentration. The maximum proliferative effect without cell death was observed at a concentration of 80 ng/ml of IL-3 (Fig. 1A and Supplementary Fig. 1) and proliferating cell nuclear antigen (PCNA) expressions as a marker for proliferation [Speir and Epstein, 1992] were increased up to 100 ng/ml of IL-3 stimulation, whereas MTT metabolic activity was reduced in 100 ng/ml. Meanwhile, migration continuously increased up to 100 ng/ml (Fig. 1B). Therefore, we continued experiments at a concentration of 80 ng/ml. To select miRNAs related to arterial remodeling in SMCs, we first searched for published papers regarding miRNAs that are related to proliferation or migration because these miRNAs are representative of arterial remodeling. Six miRNAs (miR-29b, −26a, −145, −210, and −221/222) were found to satisfy both criteria (Supplementary Fig. 2). The expression levels of the selected miRNAs were measured inIL-3-stimulated SMCs. SMC enriched with miR-145 andmiR-221/222 were examined. The miR-145 expression was continuously decreased for 48 h under IL-3 stimulation. However, miR-221/222 showed increased expression at 24 h and then decreased expression to 30% of the control at 48 h after IL-3 stimulation (data not shown). Although miR-29b showed relatively lower expression in control SMCs compared to miR-145 andmiR-221/222, the most significantly reduced expression (over 80%) was observed with IL-3 stimulation (Fig. 1C). A time-dependent expression was also investigated in IL-3-stimulated SMCs, and a continuous reduction of miR-29b expression was observed for 48 h, as shown in Figure 1D. We transfected miR-29b and measured the overexpression levels in SMCs to verify the regulation of proliferation and migration by the ectopic expression of miR-29b for the further studies (Supplementary Fig. 3).

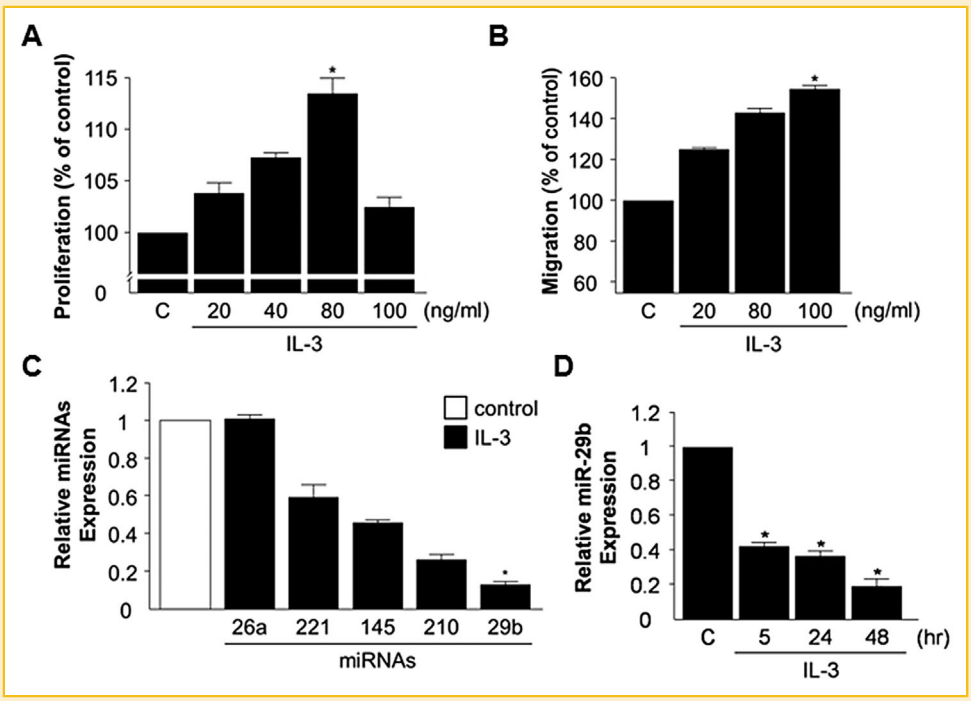

Fig. 1. Expression of microRNAs in the IL-3-stimulated SMCs. A: The effect of IL-3 on SMC proliferation was measured using an MTT assay. The SMCs were treated with 20–100 ng/ml of IL-3 for 48 h under growth conditions at 37 °C and 5% CO_2. Each experiment was performed in triplicate (n = 4). B: The effect of IL-3 on SMC migration was measured using a wound healing assay. The SMCs were treated with 20–100 ng/ml of IL-3 for 48 h (n = 5). C: Expression levels of selected microRNAs from the SMCs with or without 80 ng/ml IL-3 stimulation for 48 h; validation of microRNA expression was analyzed by real time-PCR and normalized to U6 (n = 3). After fold induction ($2^{-\Delta\Delta Ct}$) was obtained by normalization, the control value for each miRNA was modified to 1 and then values of miRNAs also were revised. D: Time-dependent effect of IL-3 on relative miR-29b expressions (n = 4). *$P < 0.05$ vs. control, C: control.

MiR-29b DIRECTLY TARGETS MCL-1 AND MMP2 IN SMCS

We searched the TargetScan program to determine the potential targets of miR-29b. Among the candidates, Mcl-1 and MMP2 are highly involved in proliferation and migration. Therefore, we checked the putative target sites of these genes with miR-29b in the 3′-UTR of rat *Mcl-1* and *MMP2* (Supplementary Fig. 4). Luciferase assay was performed to validate sequences of targets. According to the predictions based on the program, miR-29b significantly decreased the luciferase activities of *Mcl-1* and *MMP2* up to approximately 50% and 60%, respectively (Fig. 2A). Because the *Mcl-1* gene is known to be induced by IL-3 with other growth factors and cytokines, we tested whether the miR-29b can decrease the expression of Mcl-1 induced by IL-3 in SMCs. IL-3 was treated for 6 h in SMCs because Mcl-1 is known to have a protein expression half-life of 4–6 h [Mott et al., 2007]. IL-3 increased Mcl-1 expression up to 4.5-fold, and miR-29b attenuated Mcl-1 expression to approximately 30% under IL-3 stimulation (Fig. 2B). We also examined the effect of miR-29b on mRNA expression levels, in which miR-29b did not change *Mcl-1* expression level (Fig. 2C). To determine whether miR-29b can regulate MMP2 as another target of miR-29b, we also examined MMP2 expression and activation. The *MMP2* expression level was induced by IL-3 stimulation for up to 48 h (data not shown). The protein expression and activation level of MMP2 showed similar trends, and we confirmed that miR-29b selectively inhibited the expression and activation levels of MMP2 (Fig. 2D and 2E, and Supplementary Fig. 5).

MiR-29b ATTENUATES IL-3-STIMULATED PROLIFERATION AND MIGRATION BUT NOT THROUGH THE MAPK, PI3K, OR MMP9 SIGNALING PATHWAYS

In SMCs treated with 80 ng/ml of IL-3, miR-29b was overexpressed to determine whether it could inhibit the cell growth induced by IL-3 stimulation. MiR-29b significantly attenuated the SMCs proliferation and PCNA expression under IL-3 stimulation compared to IL-3-treated group (Fig. 3A and Supplementary Fig. 5). In addition, miR-29b attenuated cell cycle progression (Supplementary Fig. 6). We then examined whether miR-29b treatment can affect the activation of ERK1/2 and Akt, the upstream signaling pathway of Mcl-1, under IL-3 stimulation. IL-3 significantly increased the phosphorylation of both ERK1/2 and Akt as expected, but miR-29b did not alter the phosphorylation level of these kinases. These data demonstrate that miR-29b can target Mcl-1 but not the upstream regulators of MAPK and Akt (Fig. 3B and 3C). To test the inhibitory effect of miR-29b on IL-3-induced SMC migration, Boyden chamber and wound healing assays were performed (Fig. 4A and 4B, and Supplementary Fig. 7). MiR-29b reduced SMC migration in both

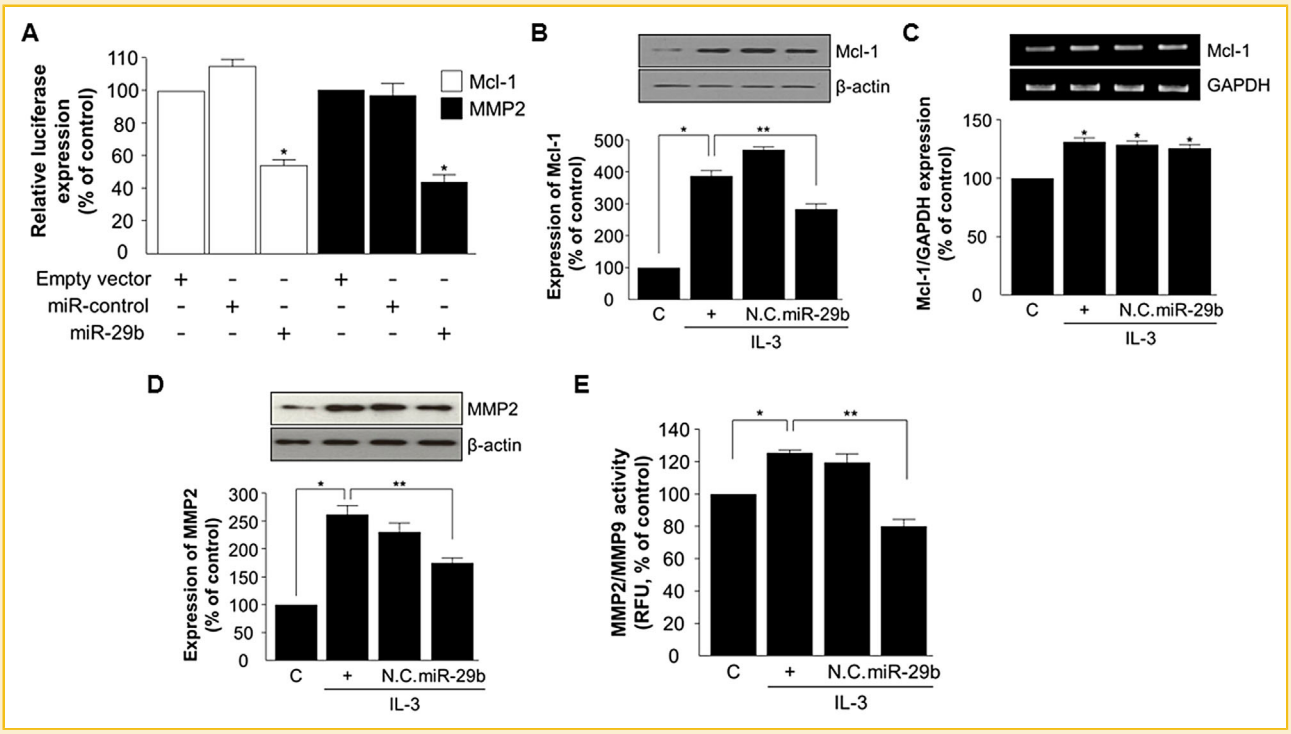

Fig. 2. The effect of miR-29b on the expression levels of Mcl-1 and MMP2 in IL-3-stimulated SMCs. A: 3′-UTR expressions of *Mcl-1* and *MMP2* were detected by the luciferase assay. The control, *Mcl-1*, or *MMP2* 3′-UTR vectors were transfected with miR-control or miR-29b. Luciferase activities were measured by a dual luciferase assay and normalized to Renilla activity. *$P < 0.05$ vs. empty vector, n = 5. B: SMCs were starved with 0.1% FBS DMEM and then 80 ng/ml of IL-3 treatment for 6 h after transfection with miR-29b. Mcl-1 expression was measured by immunoblot analysis (n = 5). C: SMCs were transfected with miR-29b, followed by IL-3 treatment for 6 h. *Mcl-1* mRNA expression was analyzed by RT-PCR and normalized to *GAPDH* (n = 3). D: SMCs were transfected with miR-29b, followed by IL-3 treatment for 48 h. MMP2 expression was analyzed by immunoblot analysis. The immune reactivity was normalized to β-actin (n = 4). E: SMCs were transfected with miR-control or miR-29b and then treated with 80 ng/ml of IL-3. The conditioned medium was harvested and subjected to InnoZyme™ Gelatinase (MMP2/MMP9) activity assay. Fluorescence measured using a fluorescence plate reader set at an excitation of 320 nm and an emission of 405 nm (n = 3). *$P < 0.05$ vs. control, **$P < 0.05$ vs. IL-3. C: control, N.C.: negative control.

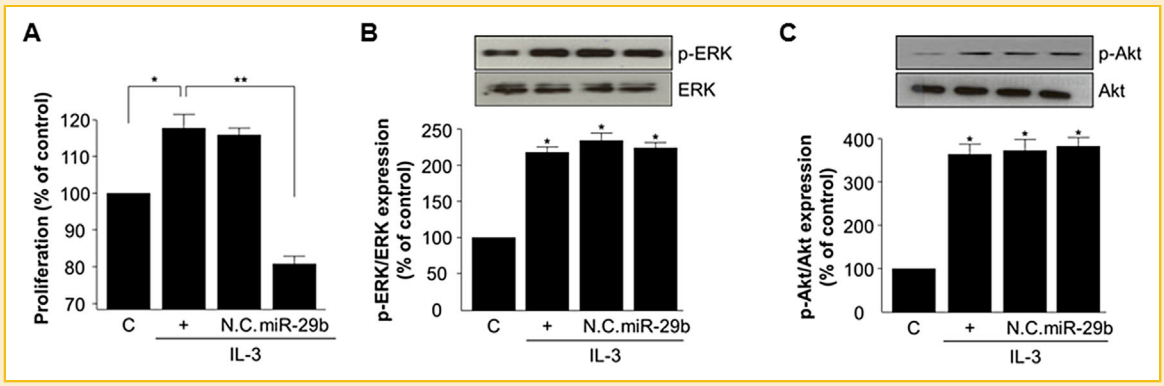

Fig. 3. The effect of miR-29b on the activity of proliferation signals at IL-3-stimulated SMCs. A: The effect of miR-29b on SMC proliferation was measured using a MTT assay. SMCs were transfected with 100 nM of miR-29b for 4 h and then treated with IL-3 for 48 h. Each experiment was performed in triplicate ($n = 5$). B: Altered phosphorylation levels of proliferation signals were assessed in IL-3-stimulated SMCs with or without miR-29b using immunoblot analysis ($n = 4$). *$P < 0.05$ vs. control, **$P < 0.05$ vs. IL-3.

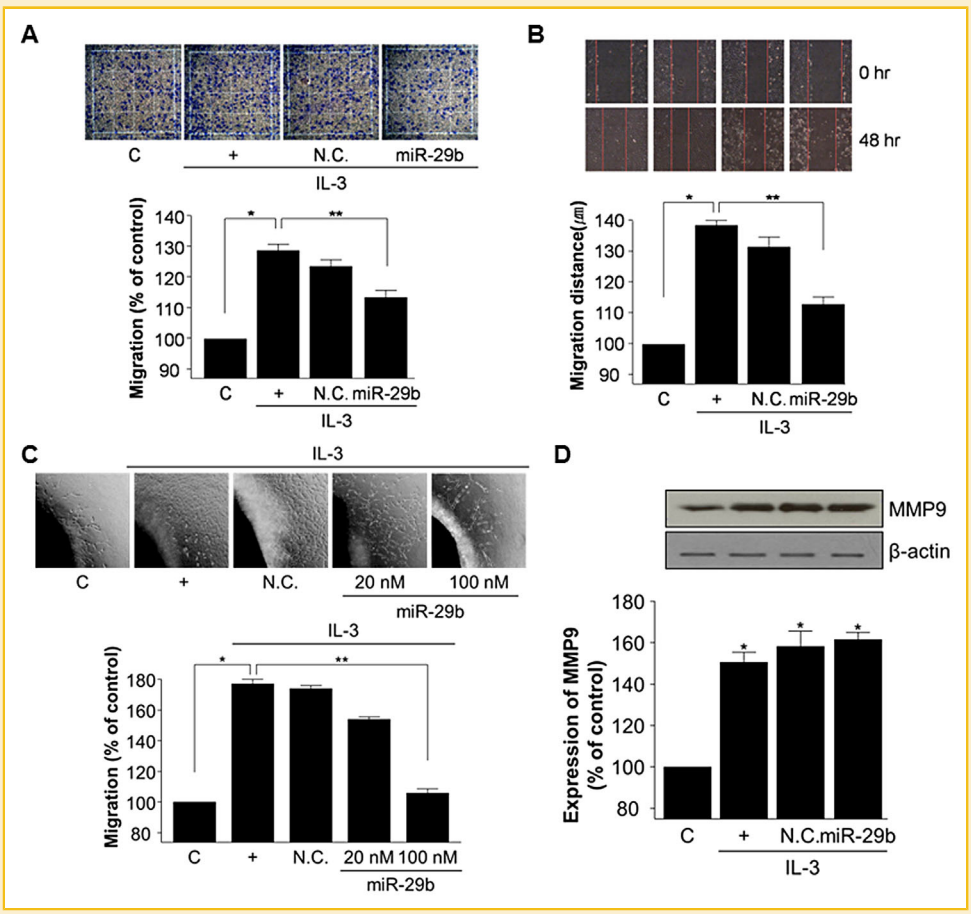

Fig. 4. The effect of miR-29b on the activity of migration at IL-3-stimulated SMCs. A: The effect of miR-29b on SMCs treated with IL-3 was measured using Boyden chambers. Migration was performed for 9 h ($n = 5$). B: MiR-29b was transfected and then IL-3 was treated for 48 h. The migration rate was investigated using a wound healing assay ($n = 3$). C: Effects of miR-29b on IL-3-induced sprout formation of aortic rings. Aortic rings (1 mm) embedded and cultured in Matrigel were starved with serum free DMEM overnight and then transfected with 100 nM of N.C. and 20 or 100 nM of miR-29b for 12 h, followed by the treatment with or without IL-3 in 10% FBS DMEM ($n = 3$). D: MiR-29b was transfected and then IL-3 was treated for 48 h. MMP9 expression was measured by immunoblot analysis and normalized to β-actin ($n = 3$). *$P < 0.05$ vs. control, **$P < 0.05$ vs. IL-3.

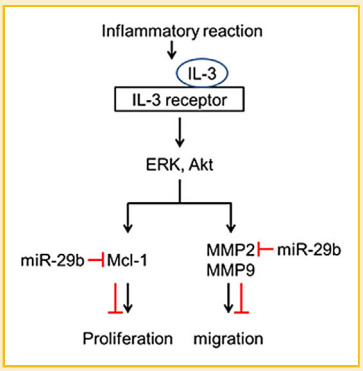

Fig. 5. Mimetic diagram of signaling pathways on miR-29b specific inhibition under IL-3 stimulation.

experiments. To confirm the inhibitory effect of miR-29b on ex vivo proliferation and migration, an aortic ring assay was performed. IL-3 increased the sprout outgrowth of aortic rings, and miR-29b inhibited this response in a dose-dependent manner (Fig. 4C). In addition to MMP2, MMP9 is an important protein involved in SMC migration. Although IL-3 induced *MMP9* expression levels in a time-dependent manner up to 48 h (data not shown), miR-29b did not inhibit the MMP9 expression level under IL-3 stimulation (Fig. 4D). Figure 5 summarizes the signaling pathways of miR-29b specific-inhibition under IL-3-stimulation. The exogenous over-expression of miR-29b attenuates IL-3-induced proliferation and migration, with Mcl-1 and MMP2 as likely targets.

OVEREXPRESSION OF MIR-29B ATTENUATES NEOINTIMAL FORMATION IN A RAT CAROTID ARTERY BALLOON INJURY MODEL

To measure the potential roles of miR-29b in a neointima formation in vivo model, we applied miR-29b to the site of injury after balloon injury. As verifications were performed two weeks after the injury, we checked whether miR-29b was successfully delivered to and active at the vascular wall by using Cy3-labeled miR-29b to visualize miR-29b. Cy3-miR-29b was detected from longitudinal and transverse strips of the carotid artery (Fig. 6A) and from the paraffin section (Fig. 6B) over the two-week period. In balloon-injured arteries, miR-29b showed the expected inhibitory effect on neointimal formation. The neointimal hyperplasia (I/M) ratio (Fig. 6C) and proliferation of neointimal region (Fig. 6D) were significantly reduced in the miR-29b-treated group. Masson's Trichrome staining indicated that interstitial collagen (blue), an important contributor for arterial remodeling [Ward et al., 2001] which accumulated after balloon injury in the N.C.-treated group, decreased by miR-29b (Fig. 6E). Because we investigated the reduced miR-29b expression and increased expressions of the targets of miR-29b in vitro, the change of endogenous miR-29b expression level was also estimated. A reduction of over 80% was observed in balloon-injured aorta tissues (Fig. 6F). Mcl-1 and MMP2 showed a marginal increase of expression in the neointimal area but were effectively repressed in the miR-29b-treated group (Supplementary Fig. 8). These results suggest that miR-29b suppressed proliferation and migration by targeting Mcl-1 and MMP2, resulting in the inhibition of the neointimal formation.

DISCUSSION

Our data show that as a stimulant, IL-3 successfully increased SMC proliferation and migration, which allowed us to investigate the corresponding mechanism (Fig. 1A and 1B). IL-3 signaling is mainly related to the signaling pathways of proliferation and the survival of kinases including, the Janus kinase (JAK), PI3K/Akt, and the MAPK kinase (MEK)/MAPK pathway [Southgate et al., 1992; George et al., 1997]. In addition, recent studies have revealed that IL-3 contributes to the stabilization of transcripts to increase cell growth in patients with leukemia [Ernst et al., 2009]. Our results indicate that IL-3 has a more effect on migration than proliferation. However, there are no existing quantitative studies which compare the effects between proliferation and migration.

Mcl-1 is involved in the downstream signaling of IL-3 stimulation and has been examined in other tissues related to proliferation. The increased expression of Mcl-1 has been shown in several tissues, such as, lymphoma and human neutrophils, to be related to vascular endothelial growth factor and other cytokines [Moulding et al., 1998; Kuramoto et al., 2002]. Mcl-1 expression is also known to be increased through MAPK and Akt signaling for proliferation and migration under IL-3 stimulation [Zhou et al., 1997; Wang et al., 2003; Le Gouill et al., 2004]. As one of Mcl-1-targeting miRs, miR-29b was demonstrated by Ru et al. [2012] to directly down-regulate the translation of Mcl-1 protein and then suppress cancer progression in prostate cancer cells and cholangiocarcinoma cell lines. In Figure 2C, we were able to confirm that the Mcl-1 transcriptional level is not affected by miR-29b. In this study, we focused on whether miR-29b is capable in reducing SMCs proliferation and migration. However, Mcl-1 has been primarily described as an important anti-apoptotic protein belonging to Bcl-2 family [Dzhagalov et al., 2007]; thus, we checked the possibility that miR-29b may induce apoptosis through the reduction of Mcl-1 protein level. In our experimental conditions, we confirmed that no significant apoptosis was induced by miR-29b (Supplementary Fig. 9). We just confirmed that S-phage cell cycle was arrested by miR-29b (Supplementary Fig. 6). These data may suggest that Mcl-1 is important for proliferation in cells and enough to regulate proliferation, but contribution is not really significant compared to cancer cells. Because there are no significant apoptosis observed from studies using SMCs, miR-29b was transfected [Du et al., 2012; Maegdefessel et al., 2012]. And also in myoblast cells, althoughmiR-29b reduced the proliferation, apoptosis did not be examined [Wei et al., 2014]. Therefore, this is still remained to be investigated why Mcl-1 did not cause apoptosis as well as studies using Mcl-1 inhibition.

Although IL-3 is known to induce proliferation and migration, mechanisms related to MMPs have not been well researched. MMPs are well known for their direct involvement in SMC migration and proliferation in experiments using MMP inhibitors and several surgical models [Southgate et al., 1992; George et al., 1997]. In the present study, we demonstrated that IL-3 can induce MMP2 and MMP9 and that miR-29b selectively reduces MMP2 (Fig. 2D and 4D,

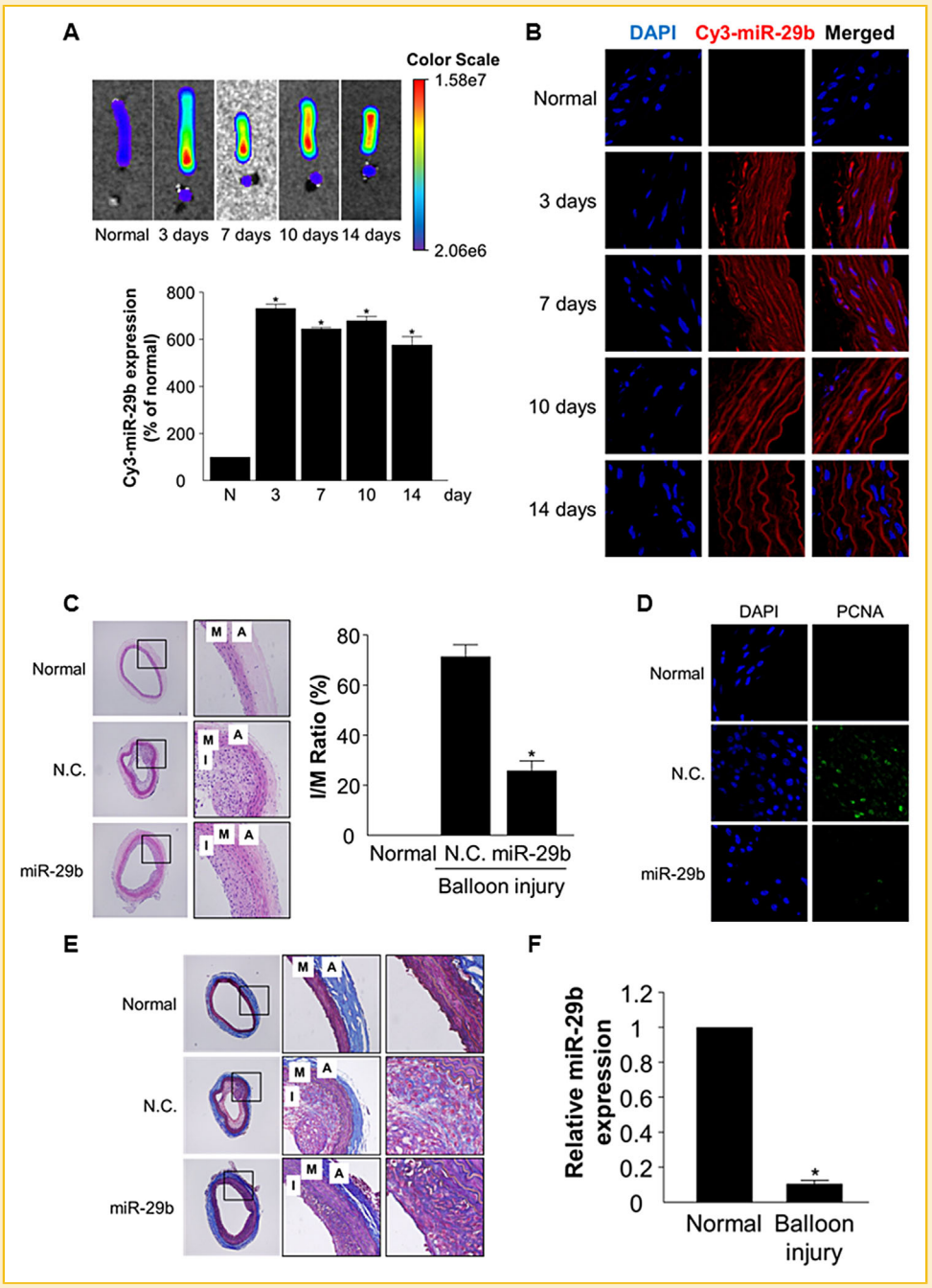

Fig. 6. The effect of miR-29b on the neointimal formation at the site of balloon-injury. A: The upper panel shows representative IVIS images from histological sections and the lower histogram shows the Cy3-miR-29b expression level (rainbow) of each normal aorta. *$P < 0.05$ vs. normal, n = 3 aortas per experimental group. B: Cy-3-miR-29b into aortas. The delivered Cy-3-miR-29b in aortas was detected by immunofluorescence. DAPI and anti-Cy3Ab were used for nuclei (blue) staining and Cy3-positive signals (red), respectively (40x magnification, n = 3 paraffin sections per experimental group). C: Ratio of neointimal to medial area (N/M) was decreased by miR-29b transfection in the balloon injury site (H&E stain). *$P < 0.05$ vs. N.C., I: Neointima, M: Media, A: Adventitia, n = 5 paraffin sections per experimental group. D: Immunofluorescent staining of aorta with or without miR-29b: PCNA. Original magnification of 40x for each plot. Blue signals represent DAPI-stained nuclei. Green signals represent PCNA (n = 3 paraffin sections per experimental group). E: Representative images taken from a Masson's trichrome–stained section (collagen is stained blue; n = 3): left panel (10x), middle panel (40x), and right panel (63x), I: Neointima, M: Media, A: Adventitia, n = 3 paraffin sections per experimental group. F: Expression level of miR-29b in balloon injury site *$P < 0.05$ vs. normal, n = 3 aorta samples per experimental group.

and Fig. 4D). In hepatocellular carcinoma, Fang et al. [2011] showed a correlation between miR-29b and MMP2 by demonstrating that miR-29b significantly suppressed angiogenesis, invasion, and metastasis in cancer by regulating MMP2 expression. Additionally, Maegdefessel et al. showed that miR-29b can down-regulate MMP2 activity and expression related to fibrosis in human aortic smooth muscle cells through TGF-β1 stimulation [Maegdefessel et al., 2012]. In contrast, Chen et al. [2011] revealed that upregulated miR-29b by oxLDL induced migration through the increase of MMP2 and MMP9 expression in human aortic SMCs. Nevertheless, most papers show that the miR-29 family can inhibit proteins that are related to migration and proliferation such as collagen, MMPs, and Mcl-1 [Sengupta et al., 2008; Steele et al., 2010]. Recently, ADAMTS-7, a metalloproteinase and a target of miR-29b, is known to have critical roles in arterial and cardiac remodeling [Du et al., 2012], but we did not focused on this study. Here, we investigated the representative signaling molecules stimulated by IL-3 to determine whether miR-29b can regulate proliferation and migration through the inhibition of its own targets. We demonstrated that miR-29b decreased Mcl-1 and MMP2 in SMCs and that this decrease is correlated with inhibition of proliferation and migration (Fig. 2 and Fig. 4).

To support the in vitro experiments, we investigated the effect of miR-29b in an in vivo balloon injury model. We examined a reduced collagen accumulation as well as MMP2 due to miR-29b treatment, which shows the anti-restenosis effects of miR-29b treatment (Fig. 6E and Supplementary Fig. 8). Although we did not confirmed in this experiment, collagens are well-known targets of miR-29b, especially type I collagen which can promote MMP-2 activation. And collagen and MMP activation has been reported that these have very important consequences in proliferation and migration [Theret et al., 2001; Li et al., 2010].

Because several cancer studies have shown that miR-29b can regulate migration, proliferation, or apoptosis, we were able to consider the capability of miR-29b to reduce the proliferation and migration processes of SMCs in pathologic conditions. Indeed, miR-29b significantly reduced the levels of Mcl-1 and MMP2 and decreased proliferation and migration. In summary, our findings demonstrated that miR-29b successfully suppressed the proliferation and migration of SMCs induced by IL-3 stimulation, probably through targeting of Mcl-1 and MMP2 in in vitro, ex vivo, and in vivo.

ACKNOWLEDGMENTS

This work was supported by grants from supported by a Korea Science and Engineering Foundation Grant funded by the Korean Government (MEST) (2014030459), a grant of the Korean Health Technology R&D Project, Ministry of Health & Welfare, Republic of Korea (A120478), and a faculty research grant of the Yonsei University College of Medicine for 2012 (8-2012-0015).

REFERENCES

Baker M,Robinson SD, Lechertier T, Barber PR, Tavora B, D′Amico G, Jones DT, Vojnovic B, Hodivala-Dilke K. 2012. Use of the mouse aortic ring assay to study angiogenesis. Nature Protocols 7:89–104.

Bernecker C, Lenz L, Ostapczuk MS, Schinner S, Willenberg H, Ehlers M, Vordenbaumen S, Feldkamp J, Schott M. 2012. MicroRNAs -146a1, -155 2, -200a1 are regulated in autoimmune thyroid diseases Thyroid 22:1294–1295.

Brizzi MF, Formato L, Dentelli P, Rosso A, Pavan M, Garbarino G, Pegoraro M, Camussi G, Pegoraro L. 2001. Interleukin-3 stimulates migration and proliferation of vascular smooth muscle cells - A potential role in atherogenesis. Circulation 103:549–554.

Chen KC, Wang YS, Hu CY, Chang WC, Liao YC, Dai CY, Juo SH. 2011. OxLDL up-regulates microRNA-29b, leading to epigenetic modifications of MMP-2/MMP-9 genes: A novel mechanism for cardiovascular diseases. FASEB J 25:1718–1728.

Costa MA, Simon DI. 2005. Molecular basis of restenosis and drug-eluting stents. Circulation 111:2257–2273.

Du Y, Gao C, Liu Z, Wang L, Liu B, He F, Zhang T, Wang Y, Wang X, Xu M, Luo GZ, Zhu Y, Xu Q, Wang X, Kong W. 2012. Upregulation of a disintegrin and metalloproteinase with thrombospondin motifs-7 by miR-29 repression mediates vascular smooth muscle calcification. Arterioscler Thromb Vasc Biol 32:2580–2588.

Dzhagalov I, St John A, He YW. 2007. The antiapoptotic protein Mcl-1 is essential for the survival of neutrophils but not macrophages. Blood 109:1620–1626.

Ernst J, Ghanem L, Bar-Joseph Z, McNamara M, Brown J, Steinman RA. 2009. IL-3 and oncogenic Abl regulate the myeloblast transcriptome by altering mRNA stability. PLoS One 4:e 7469.

Fang JH, Zhou HC, Zeng C, Yang J, Liu Y, Huang X, Zhang JP, Guan XY, Zhuang SM. 2011. MicroRNA-29b suppresses tumor angiogenesis, invasion, and metastasis by regulating matrix metalloproteinase 2 expression. Hepatology 54:1729–1740.

Fichtlscherer S, De Rosa S, Fox H, Schwietz T, Fischer A, Liebetrau C, Weber M, Hamm CW, Roxe T, Muller-Ardogan M, Bonauer A, Zeiher AM, Dimmeler S. 2010. Circulating microRNAs in patients with coronary artery disease. Circ Res 107:677–257.

George SJ, Zaltsman AB, Newby AC. 1997. Surgical preparative injury and neointima formation increase MMP-9 expression and MMP-2 activation in human saphenous vein. Cardiovasc Res 33:447–459.

Hwang KC, Lee KH, Jang Y, Yun YP, Chung KH. 2002. Epigallocatechin-3-gallate inhibits basic fibroblast growth factor-induced intracellular signaling transduction pathway in rat aortic smooth muscle cells. J Cardiovasc Pharmacol 39:271–277.

Kairouz V, Lipskaia L, Hajjar RJ, Chemaly ER. 2012. Molecular targets in heart failure gene therapy: Current controversies and translational perspectives. Ann N Y Acad Sci 1254:42–50.

Kasinski AL, Slack FJ. 2012. MiRNA-34 prevents cancer initiation and progression in a therapeutically resistant K-ras and p53-induced mouse model of lung adenocarcinoma. Cancer Res 72:5576–5587.

Kumar A, Hoover JL, Simmons CA, Lindner V, Shebuski RJ. 1997. Remodeling and neointimal formation in the carotid artery of normal and P-selectin-deficient mice. Ciculation 96:4333–4342.

Kuramoto K, Sakai A, Shigemasa K, Takimoto Y, Asaoku H, Tsujimoto T, Oda K, Kimura A, Uesaka T, Watanabe H, Katoh O. 2002. High expression of MCL1 gene related to vascular endothelial growth factor is associated with poor outcome in non-Hodgkin′s lymphoma. Brit J Haematol 116:158–161.

Kwon C, Han Z, Olson EN, Srivastava D. 2005. MicroRNA1 influences cardiac differentiation in drosophila and regulates notch signaling. Proc Natl Acad Sci U S A 102:18986–18991.

Le Gouill S, Podar K, Amiot M, Hideshima T, Chauhan D, Ishitsuka K, Kumar S, Raje N, Richardson PG, Harousseau JL, Anderson KC. 2004. VEGF induces Mcl-1 up-regulation and protects multiple myeloma cells against apoptosis. Blood 104:2886–2892.

Lee ST, Chu K, Jung KH, Kim JH, Huh JY, Yoon H, Park DK, Lim JY, Kim JM, Jeon D, Ryu H, Lee SK, Kim M, Roh JK. 2012. MiR-206 regulates

brain-derived neurotrophic factor in Alzheimer disease model. Ann Neurol 72:269–277.

Li A, Zhou T, Guo L, Si J. 2010. Collagen type I regulates beta-catenin tyrosine phosphorylation and nuclear translocation to promote migration and proliferation of gastric carcinoma cells. Oncol Rep 23:1247–1255.

Liu XJ, Cheng YH, Chen XW, Yang J, Xu L, Zhang CX. 2011. MicroRNA-31 regulated by the extracellular regulated kinase is involved in vascular smooth muscle cell growth via large tumor suppressor homolog 2. J Biol Chem 286:42371–42380.

Maegdefessel L, Azuma J, Toh R, Merk DR, Deng A, Chin JT, Raaz U, Schoelmerich AM, Raiesdana A, Leeper NJ, McConnell MV, Dalman RL, Spin JM, Tsao PS. 2012. Inhibition of microRNA-29b reduces murine abdominal aortic aneurysm development. J Clin Invest 122:497–506.

McDonald RA, Hata A, MacLean MR, Morrell NW, Baker AH. 2012. MicroRNA and vascular remodelling in acute vascular injury and pulmonary vascular remodelling. Cardiovasc Res 93:594–604.

Mott JL, Kobayashi S, Bronk SF, Gores GJ. 2007. Mir-29 regulates Mcl-1 protein expression and apoptosis. Oncogene 26:6133–6140.

Moulding DA, Quayle JA, Hart CA, Edwards SW. 1998. Mcl-1 expression in human neutrophils: Regulation by cytokines and correlation with cell survival. Blood 92:2495–2502.

Nazari-Jahantigh M, Wei Y, Schober A. 2012. The role of microRNAs in arterial remodelling. Thromb Haemost 107:611–618.

Ounzain S, Crippa S, Pedrazzini T. 2012. Small and long non-coding RNAs in cardiac homeostasis and regeneration Biochim Biophys Acta 1833: 923–933.

Ru P, Steele R, Newhall P, Phillips NJ, Toth K, Ray RB. 2012. MiRNA-29b suppresses prostate cancer metastasis by regulating epithelial-mesenchymal transition signaling. Mol Cancer Therap 11:1166–1173.

Rudolph T, Schaps KP, Steven D, Koester R, Rudolph V, Berger J, Terres W, Meinertz T, Kaehler J. 2009. Interleukin-3 is elevated in patients with coronary artery disease and predicts restenosis after percutaneous coronary intervention. Int J Cardiol 132:392–397.

Schmitt MJ, Margue C, Behrmann I, Kreis S. 2012. miRNA -29: A microRNA family with tumor-suppressing and immune-modulating properties Curr Mol Med 13:572–585.

Sengupta S, den Boon JA, Chen IH, Newton MA, Stanhope SA, Cheng YJ, Chen CJ, Hildesheim A, Sugden B, Ahlquist P. 2008. MicroRNA 29c is down-regulated in nasopharyngeal carcinomas. Pro Natl Acad Sci USA 105: 5874–5878.

Smith TP. 2002. Atherosclerosis and restenosis: An inflammatory issue. Radiology 225:10–12.

Southgate KM, Davies M, Booth RFG, Newby AC. 1992. Involvement of extracellular-matrix-degrading metalloproteinases in rabbit aortic smooth-muscle cell-proliferation. Biochem J 288:93–99.

Speir E, Epstein SE. 1992. Inhibition of smooth muscle cell proliferation by an antisense oligodeoxynucleotide targeting the messenger RNA encoding proliferating cell nuclear antigen. Circulation 86:538–547.

Steele R, Mott JL, Ray RB. 2010. MBP-1 upregulates miR-29b that represses Mcl-1, collagens, and matrix-metalloproteinase-2 in prostate cancer cells. Genes Cancer 1:381–387.

Talasila A, Yu H, Ackers-Johnson M, Bot M, van Berkel T, Bennett M, Bot I, Sinha S. 2013. Myocardin regulates vascular response to injury through mir-24/-29a and platelet-derived growth factor receptor beta. Arterioscler Thromb Vasc Biol 33:2355–2365.

Theret N, Musso O, Turlin B, Lotrian D, Bioulac-Sage P, Campion JP, Boudjema K, Clement B. 2001. Increased extracellular matrix remodeling is associated with tumor progression in human hepatocellular carcinomas. Hepatology 34:82–88.

Voehringer D. 2012. Basophil modulation by cytokine instruction. Eur J Immunol 42:2544–2550.

Wang C, Gao C, Zhuang JL, Ding C, Wang Y. 2012a. A combined approach identifies three mRNAs that are down-regulated by microRNA-29b and promote invasion ability in the breast cancer cell line MCF-7. J Cancer Res Clin Oncol 138:2127–2136.

Wang JM, Lai MZ, Yang-Yen HF. 2003. Interleukin-3 stimulation of mcl-1 gene transcription involves activation of the PU.1 transcription factor through a p38 mitogen-activated protein kinase-dependent pathway. Mol Cell Biol 23:1896–1909.

Wang YS, Wang HY, Liao YC, Tsai PC, Chen KC, Cheng HY, Lin RT, Juo SH. 2012b. MicroRNA-195 regulates vascular smooth muscle cell phenotype and prevents neointimal formation. Cardiovasc Res 95:517–526.

Ward MR, Kanellakis P, Ramsey D, Funder J, Bobik A. 2001. Eplerenone suppresses constrictive remodeling and collagen accumulation after angioplasty in porcine coronary arteries. Circulation 104:467–472.

Zhou SY, Baltimore D, Cantley LC, Kaplan DR, Franke TF. 1997. Interleukin 3-dependent survival by the Akt protein kinase. Pro Natl Acad Sci USA 94:11345–11350.

SUPPORTING INFORMATION

Additional supporting information may be found in the online version of this article at the publisher's web-site.